

Coherent UHF Radar for Ice Detection

June 2003

C-CORE Contract Report R-03-022-099



This page is intentionally left blank

Coherent UHF Radar For Ice Detection

Version 1.0

Prepared for:

Regional Citizens' Advisory Council (RCAC)
PO Box 3089
Valdez, AK 99686

Prepared by:

C-CORE

C-CORE Report:

R-03-022-099

June 2003



C-CORE
Captain Robert A. Bartlett Building
Morrissey Road, St. John's, NL
Canada A1B 3X5

T: (709) 737-8354
F: (709) 737-4706

Info@c-core.ca
www.c-core.ca

The correct citation for this report is:

Rowsell, D., Tarrant, S., and Power, D. (2003). "Coherent UHF Radar for Ice Detection", Contract Report R-03-022-099, v1.0, June, 2003.

Project Team

Dean Rowsell

Stefan Tarrant

Des Power (Project Manager)

Gerry Piercey

EXECUTIVE SUMMARY

The Regional Citizens' Advisory Council (RCAC), of Valdez, Alaska, has a mandate to provide enhancements in the detection of navigation hazards—particularly icebergs—in the traffic lanes of Prince William Sound. It is widely recognized that the detection of growlers and bergy bits under moderate to high sea states, or in pack ice, is outside the capabilities of current marine radar technologies. The C-CORE Coherent UHF Radar has been developed with funding from RCAC as an important component in an ice warning system to help fulfill their ice management responsibilities.

The coherent radar, is intended for the detection of small targets in the presence of significant clutter caused by rough seas or pack ice. A prototype system was brought to Valdez, Alaska, in April 2003, for a field evaluation. The radar utilizes stepped frequency modulation (SFM) as a means of transmitting a low-power, wide-pulse signal to achieve a resolution similar to traditional high-power, narrow-pulse systems. Enhanced signal processing is possible due to the coherent nature of the design, thereby permitting novel approaches to target detection in the presence of clutter. The UHF radar was designed to operate in two frequency ranges for comparison—L-band (750MHz - 800MHz) and S-Band (2400MHz – 2450MHz). Custom, narrow beamwidth waveguide antennas were also designed to aid in target isolation. A PC graphical user interface (GUI) provided control over all features of the radar and maintained records for every radar transmission.

The objectives of the field program, which extended over a period of two weeks, were to: evaluate the effectiveness of SFM; perform comparisons between L-band and S-band; evaluate the custom waveguide antenna design; and, investigate the usefulness of the radar as a complement to the existing SeaScan™ system that has been installed and is now operating on Reef Island. The field program took place aboard the research vessel Auklet in order to quickly move to the location of prospective radar targets. Installation aboard this vessel went smoothly, and the support of this vessel for further work is highly recommended.

Two particular technical problems narrowed the scope and range of targets that could be used in the assessment: carrier feed-through between the transmitter and receiver; and temporary loss of gain in the demodulator following each signal burst. These problems were well-characterized during the study, which will enable a prediction of system performance upon remedy of these problems. The work also highlighted further system improvements that will improve both the range and resolution capabilities of the system. In particular, an embedded microcontroller would provide the precise timing

requirements for a multiple sweep transmission, thus enabling significant improvement of target detection range and/or small target detection. Further focus on signal design that is amenable to enhanced Doppler processing will also be possible with a multi-sweep capability.

Data for analysis was acquired from both icebergs and navigation buoys. Due to non-ideal weather conditions for generating clutter (it was too calm) and the two identified technical problems, all of the experimental objectives were not met. Small-target detection will improve with the remedy of the identified technical problems; however, performance measures across a wide range of clutter conditions will remain unknown until further field work can be conducted under prescribed conditions. The superior resolution available through application of SFM was demonstrated, as well as the ability to detect very weak radar returns. The custom antenna met its design requirements, both electrically and mechanically. Notably, the entire development program demonstrated that coherent SFM methodology can be introduced to marine radar in a very cost-effective manner. The wireless technologies available today are of tremendous benefit to the development of advanced radar technologies, and continued improvement in this regard should be expected, in terms of cost and performance.

The next phase should incorporate the needed system modifications identified during this study, and repeat the field program under sea conditions that present significant clutter to the radar. To that end, C-CORE remains confident that coherent processing in the UHF band is key to surpassing the capabilities of existing marine radar in the detection of small targets in the presence of clutter, and will endeavor to forge ahead with this technology.

TABLE OF CONTENTS

1	Introduction.....	1
2	Functional Description of RADAR	2
2.1	System Overview	2
2.2	Signal Design	2
2.3	Hardware Description.....	4
2.4	Antennas.....	5
2.5	Graphical User Interface.....	7
3	Field Program.....	8
3.1	Study Area.....	8
3.2	Objectives.....	9
3.2.1	<i>Evaluate Effectiveness of Stepped Frequency Modulation</i>	9
3.2.2	<i>Compare Two Different Ranges Within the UHF Band</i>	9
3.2.3	<i>Evaluate Custom Waveguide Antenna Design</i>	9
3.2.4	<i>Evaluate UHF Radar as a Complement to the SeaScan[®] System</i>	10
3.3	Installation and Set-Up.....	10
3.4	Evaluation Activities and Resulting Data	13
3.4.1	<i>Middle Rock Navigation Marker</i>	14
3.4.2	<i>Bligh Reef RACON</i>	17
3.4.3	<i>Iceberg Near Point Freemantle</i>	18
3.4.4	<i>Glacier Island from Long Range</i>	20
3.4.5	<i>Experimental Summary</i>	20
4	Data Analysis and Simulation.....	22
4.1	Radar Model.....	22
4.2	Doppler Processing	22
5	Conclusions and Recommendations	25
	References	27
	APPENDIX A – Graphical User Interface	28
	APPENDIX B – Vessel Route	30

LIST OF TABLES

Table 2-1 – Frequency Ranges of Operation.....	2
Table 2-2 – Signal Specifications	3
Table 2-3 – Antenna Specifications	7

LIST OF FIGURES

Figure 2-1 – SFM Description.....	3
Figure 2-2 – Simplified Block Diagram.....	4
Figure 2-3 – Radar Front Panel.....	5
Figure 2-4 – Antenna Assembly	6
Figure 2-5 – Waveguide Antennas.....	7
Figure 3-1 – Map of Study Area	8
Figure 3-2 – The Auklet.....	11
Figure 3-3 – Transceiver Installation.....	11
Figure 3-4 – Wheelhouse Configuration.....	12
Figure 3-5 – Receive Monopole	13
Figure 3-6 – Middle Rock Navigation Marker	15
Figure 3-7 – Middle Rock, Raw Uncompressed Data	16
Figure 3-8 – Middle Rock, Pulse-Compressed Output	16
Figure 3-9 – Bligh Reef RACON	17
Figure 3-10 – Bligh Reef RACON, Pulse-Compressed Output	18
Figure 3-11 – Iceberg near Point Freemantle (Glacier Island in Background).....	19
Figure 3-12 – Iceberg near Point Freemantle, Pulse-Compressed Output	19
Figure 3-13 – Glacier Island, Pulse-Compressed Output	20
Figure 4-1 – Simulated Pulse-Compressed Output.....	22

1 INTRODUCTION

Following the Exxon Valdez disaster of 1989 in Alaska, the Prince William Sound Regional Citizens' Advisory Council (RCAC) was established to promote an environmentally safe operation of both the oil tankers in Prince William Sound (PWS) and the pipeline terminal in Valdez. A key activity in their work is the detection of navigation hazards in the traffic lanes of Prince William Sound. There is a *notion*, that is consistent with discussions with many mariners operating in iceberg frequented waters, that "the major gap in the capabilities of current technology is in the detection of growlers and bergy bits under moderate to high sea states or in pack ice" (Rossiter 1995). In response to this notion, the C-CORE Coherent UHF Radar has been developed, with the financial support of RCAC, as an important component in ice warning systems. The purpose of the project has been to investigate the application of the coherent UHF radar to the detection of small icebergs, particularly when the sea state is severe. Earlier work pointed to the potential of utilizing the UHF band, due to diminished levels of sea clutter in the radar return and the favorable propagation characteristics of the UHF band compared with X-band. In order to achieve resolution comparable to (or surpassing) X-band systems, a wide-band, coherent system was necessary to take advantage of processing gain.

A two-week field program took place in Alaska during April 2003, and comprised an evaluation of the UHF radar prototype in the presence of typical ice conditions in the traffic lanes of Prince William Sound. This report will highlight this field work and the results as well as some general design issues. The report will describe how this work has been an important building block towards a fully operational system.

2 FUNCTIONAL DESCRIPTION OF RADAR

2.1 System Overview

The coherent nature of the UHF radar simply means that the signal transmitted by the antenna is derived from a highly stable oscillator, and the same oscillator is used by the receiver to perform detection of the radar backscatter from targets. Standard marine radars use unstable magnetron transmitters that limit processing gains of a multiple return configuration.

There are essentially two ways to achieve fine target resolution with radar, for reasonable cost: (1) transmit a short high-power pulse using a magnetron, or (2) transmit a long low-power coherent pulse, or series of pulses, that sweeps a wide range of frequencies. Each solution has its own particular technical and economical benefits and drawbacks (which are beyond the scope of this report), but for this work, the second method was chosen to achieve a low-cost solution that makes up for the lack of transmitter power through sophisticated signal design and processing.

The UHF band spans the frequency range from 300MHz to 3GHz. To achieve a resolution comparable to the best non-coherent radar (5m), a bandwidth of only 30MHz is required; therefore, it was decided to exploit two different frequency ranges within the UHF band, as shown in Table 2-1. The choice of two bands provided the means to determine how frequency-dependent performance factors such as clutter, effective target size, propagation loss, noise and sensitivity might affect overall target detectability.

Table 2-1 – Frequency Ranges of Operation

Band	Nominal Frequency Range
L-Band	750 – 800 MHz
S-Band	2400 – 2450 MHz

2.2 Signal Design

As stated previously, the signal design for the coherent radar took the form of a relatively long and low-power pulse, and swept a range of frequencies up to a 50MHz bandwidth. A well-known form of signal processing known as pulse compression was applied in order to convert the wide, low-power pulse into an energy-equivalent narrow, high-power pulse, thereby enhancing signal detectability and target resolution. The same concept is applied in Global Positioning Systems to detect very weak signals transmitted over a great distance. There are several schemes to choose from in this regard; however,

stepped frequency modulation (SFM) was chosen because it offered the simplest means of generation and it is well-suited to a mono-static antenna configuration (i.e. the same antenna is used for transmission and reception). An SFM signal is depicted in Figure 2-1, and simply comprised a series of equally spaced, equal-width pulses, with the frequency of each pulse incrementing linearly until the entire range of frequencies is covered. The limiting factor for bandwidth is the antenna. Because a physically different antenna was designed for L-band and S-band, each had its own particular bandwidth requirements. Additionally, various sub-components, such as the power amplifier, had different functional specifications within each band. The specifications for the coherent radar for both L-band and S-band are given in Table 2-2.

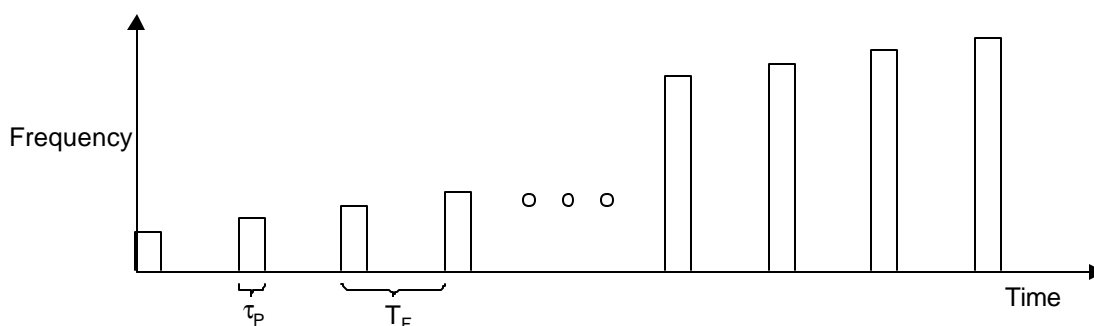


Figure 2-1 – SFM Description

Table 2-2 – Signal Specifications

Specification	L-Band	S-Band	Units
Start Frequency	757	2405	MHz
Stop Frequency	782	2439	MHz
Bandwidth	25	34	MHz
Target Resolution	6	4.4	meters
Frequency Step	0.1	0.1	MHz
Repetition Period (T_F)	100	100	μ Sec
Number Pulses (N_p)	251	341	n/a
Pulse Width (τ_p)	10	10	μ Sec
Peak Transmit Power	140	65	Watts

2.3 Hardware Description

A simplified block diagram of the system is shown in Figure 2-2, which depicts the dual-band and coherent nature of the design. Both transmitter and receiver portions of the system were designed so that either S-band or L-band could be easily chosen through a switch in the PC interface. This was an important design consideration as it provided a means to collect data on both bands from a particular target within a short time interval, thus mitigating the effects of changing environmental factors when making a comparison between the two bands.

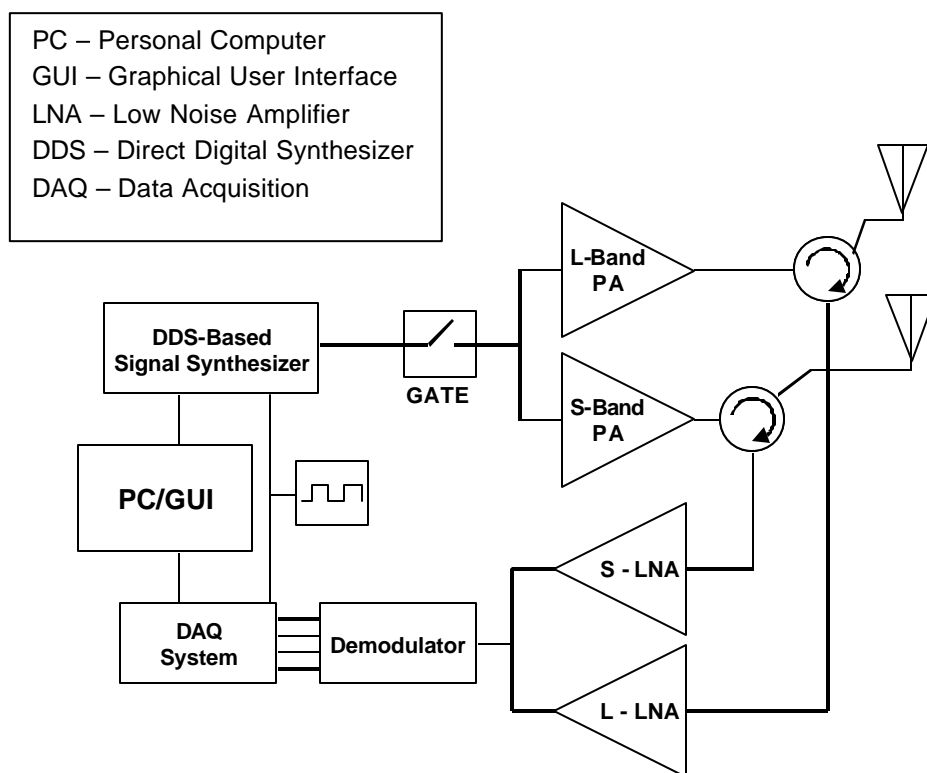


Figure 2-2 – Simplified Block Diagram

The system was designed in a modular fashion to isolate the five main components: transmitter, receiver, power amplifier, data acquisition and power supply. All components were housed in enclosures conforming to a standard 19-inch rack to facilitate shipping and installation on the research vessel. The front panel of the coherent UHF radar is pictured in Figure 2-3. Complete system control was provided through a PC graphical user interface (GUI), described in section 2.5.



Figure 2-3 – Radar Front Panel

2.4 Antennas

A custom waveguide antenna was designed for each of the two transmission bands, with a coaxial feed from the transceiver system. The antennas performed both the transmit and receive functions. An isometric drawing of the antenna assembly is shown in Figure 2-4. Figure 2-5 shows the two antennas mounted on the research vessel. The smaller of the two is the S-band antenna. Some specifications for the antenna are given in Table 2-3.

The antenna assembly was not motor driven, but rather rotated by hand from inside the vessel. A motor driven antenna was unnecessary for the field evaluation since it does nothing to assess the capabilities of the technology being investigated—it only provides full spatial coverage that would be more applicable to a fully operational system.

A usual requirement for a marine radar is that the antenna beam-pattern exhibit fine azimuthal resolution, or beamwidth, for improved target spatial isolation of targets. For

the custom design, this requirement was fulfilled through the use of multiple slots placed at appropriate intervals along the face of each antenna. This effectively increases the aperture of the antenna, thereby reducing its beamwidth. The *effective* aperture is a function of the frequency; so since both S-band and L-band antennas are similar in length, but there is a factor of three difference between the nominal transmission frequencies in each case, the effective aperture for the L-band antenna is three times shorter than that of the S-band antenna. Consequently, the beamwidth of the L-band antenna is much wider than its counterpart, as reflected by the specifications in Table 2-3. A longer L-band antenna would have been very restrictive from both shipping and installation perspectives. The necessary compromise when operating at L-band was to carefully select targets that were spatially isolated in a manner that left no ambiguities in identifying targets in the radar return.

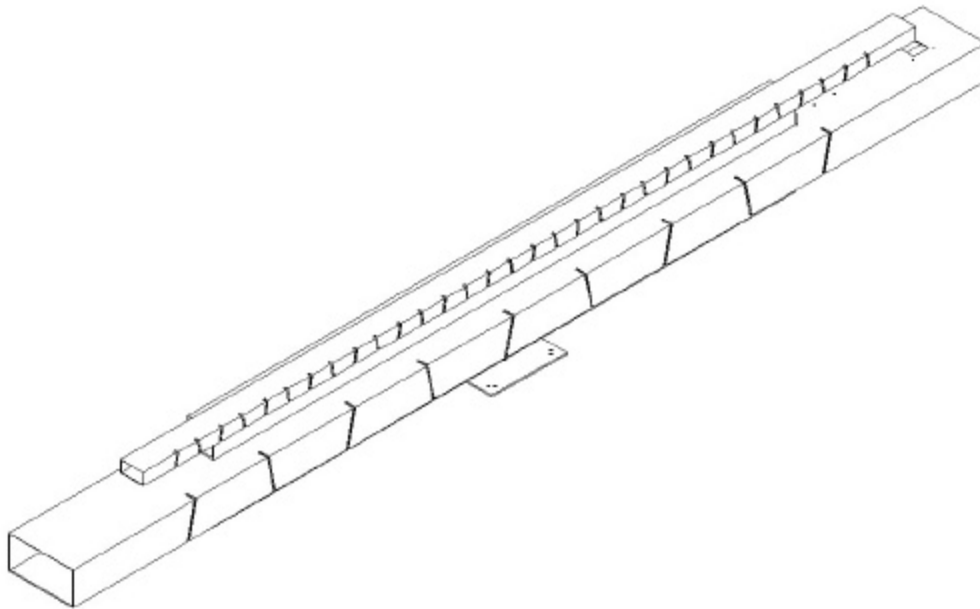


Figure 2-4 – Antenna Assembly



Figure 2-5 – Waveguide Antennas

Table 2-3 – Antenna Specifications

Specification	L-Band	S-Band	Units
Length	3.64	3.08	meters
Bandwidth (VSWR 2:1)	17.3	34.2	MHz
Bandwidth (VSWR 3:1)	25.5	43.2	MHz
Beamwidth	20	4	°
Gain	15	21	dB
Maximum Sidelobe Level	-13	-13	dB

2.5 Graphical User Interface

All of the parameters of the radar were controlled from a PC-based graphical user interface (GUI). The GUI is shown in Appendix A. Many features of the GUI are beyond the minimum requirements for field operation of the radar, but are included to facilitate laboratory testing and evaluation as well as field diagnostics. The GUI also maintained a log file into which notes corresponding to each radar transmission could be conveniently stored. Filenames were generated automatically according to date and time of day, and an '.ini' file was saved for each data record that captured the current radar settings for the corresponding transmission.

3 FIELD PROGRAM

3.1 Study Area

From past experience, due to the unpredictable availability of viable iceberg targets, it was decided to conduct the field evaluation aboard a vessel. This enabled the research staff to cruise and find the most useful radar targets. The research vessel Auklet was chartered for this purpose. Referring to Figure 3-1, most icebergs in the Valdez Arm region originate from Columbia Glacier; therefore, the most likely area to find iceberg targets was the traffic lane in Valdez Arm and the adjacent Columbia Bay region.

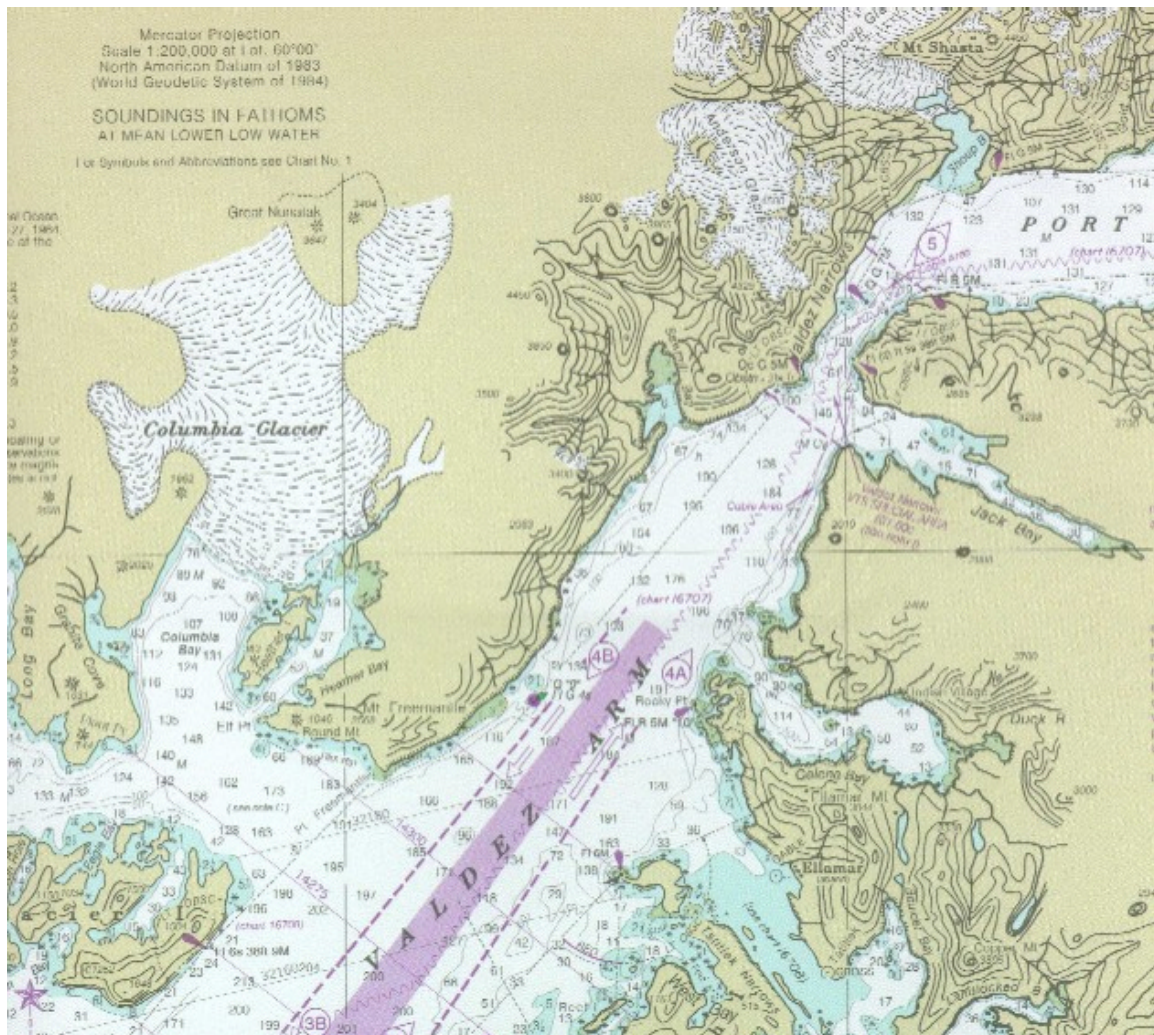


Figure 3-1 – Map of Study Area

3.2 Objectives

The following sub-sections summarize the primary objectives of the field exercise.

3.2.1 Evaluate Effectiveness of Stepped Frequency Modulation

The signal design employed in the UHF radar was simulated extensively prior to the prototype development and construction. This simulation demonstrated that pulse compression, and thus enhanced signal detectability and improved target resolution, is achievable with the SFM design. However, application to a real physical system is always subject to influences that are difficult to model such as clock jitter, non-linearity's, propagation (environmental) effects, and non-uniform output power. Therefore, the primary goal of this field exercise was to evaluate the performance of the signal design in the real world compared with the model.

3.2.2 Compare Two Different Ranges Within the UHF Band

As described above, the UHF radar was designed around two specific frequency ranges—L-band and S-band. This was important because many factors that influence target detectability are frequency dependent, such as sea clutter, noise, target strength, and propagation. An objective of the field program was therefore to collect data from targets and sea clutter on both bands (almost simultaneously), to assess performance differences between the two bands.

3.2.3 Evaluate Custom Waveguide Antenna Design

Being their first introduction to the field, the custom antennas needed to be evaluated from both mechanical and electrical perspectives. It was important to assess the mechanical soundness of the design in consideration of future deployments of the system. Although the antenna was tested electrically before shipping to Alaska, it was also important to assess its performance when installed on the research vessel and its constituent structures.

The compatibility of the SFM waveform with relatively narrowband antennas was also an important issue. If the SFM waveform worked well with the custom waveguide antenna, then it would also work well with standard radar scanners (also waveguide-based)—thus reducing the development cost and complexity of a commercial coherent UHF radar.

3.2.4 Evaluate UHF Radar as a Complement to the SeaScan™ System

The SeaScan™ system is a radar post-processor (for further details, see Chapter 5), which is installed and successfully operating from a radar site on Reef Island, PWS. It is also the ice radar processor installed on the Terra Nova Floating, Production, Storage and Offloading vessel (FPSO), the future White Rose FPSO, and the drill rigs Henry Goodrich and Erik Raude. The coherent UHF radar was conceived as a complement to the SeaScan™ system by improving the underlying radar technology to enable the detection of very small slow-moving targets, such as small icebergs, not visible on standard magnetron-based (non-coherent) pulsed radar systems. Therefore, an objective of this field program was to assess the types and sizes of radar targets that are identifiable with the coherent UHF radar and compare this with the capabilities of the existing SeaScan™ installation.

3.3 Installation and Set-Up

The field program commenced on April 1, 2003 in Valdez, Alaska. The first few days involved installation and set-up of the radar system aboard the Auklet, shown in Figure 3-2. The equipment rack containing the transmitter and receiver was situated in the research office area in the forecastle of the vessel, as shown in Figure 3-3. For future consideration, the 19" rack enclosure that housed the radar components did not fit through the main cabin door of the Auklet, nor through the stairway to the forecastle. As a result, the radar components and the enclosure had to be disassembled on deck and reassembled in the forecastle.



Figure 3-2 – The Auklet

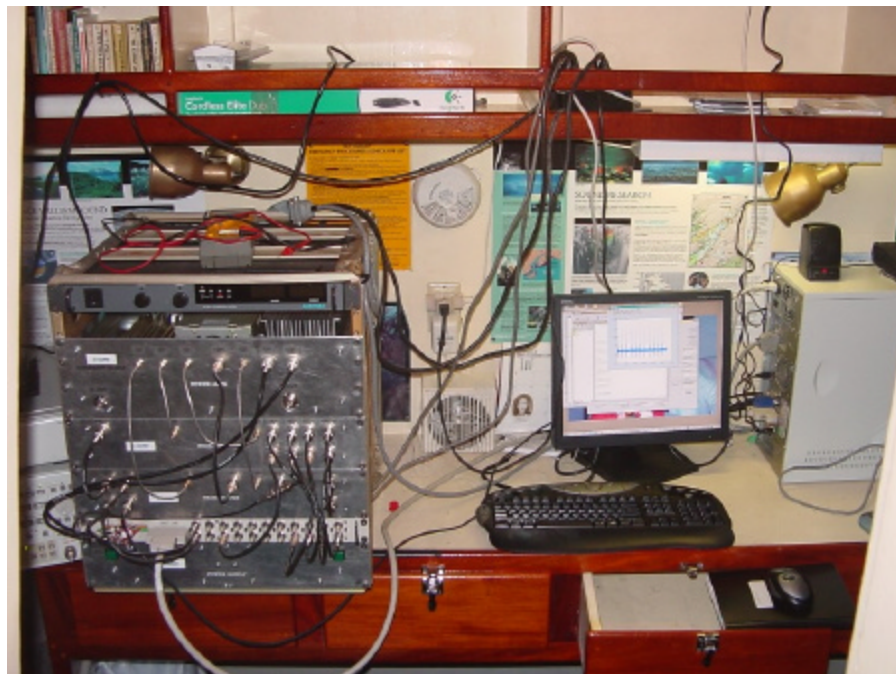


Figure 3-3 – Transceiver Installation

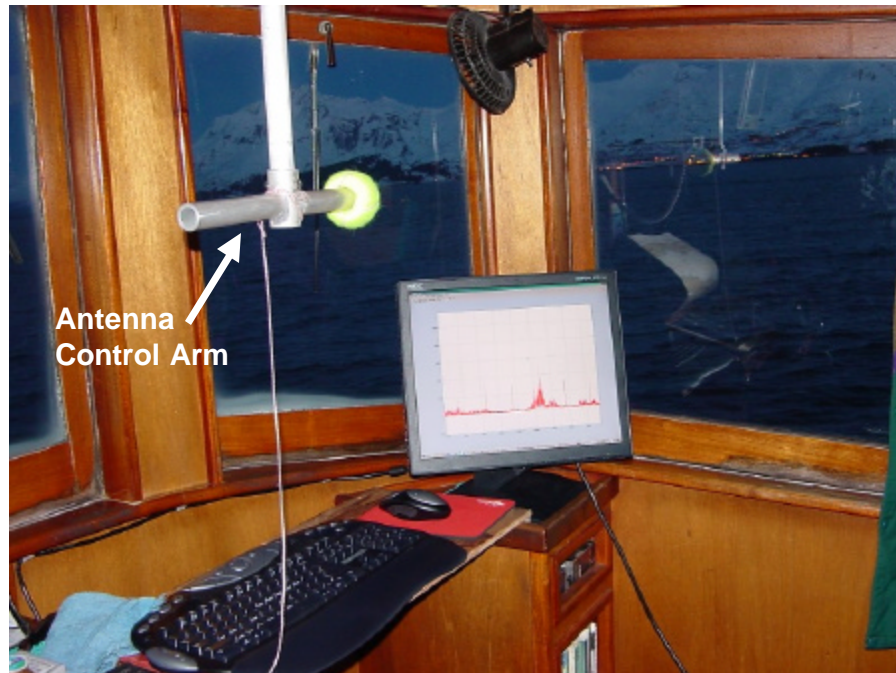


Figure 3-4 – Wheelhouse Configuration

A wireless keyboard and mouse provided the option to use the GUI and exercise complete control over the radar system from the wheelhouse, as shown in Figure 3-4. This picture also shows the control arm for the antenna which is conveniently located so the GUI can be operated while orienting the antenna towards a target of interest.

Low-loss semi-flexible coaxial cable (Heliax™) was routed between the transceiver and the two antennas located atop the wheelhouse (previously shown in Figure 2-5). Throughout the field program, there was a requirement to operate the system in a bi-static configuration to mitigate the effects of carrier feed-through, whereby a separate monopole antenna was used to receive the backscatter. This antenna was located on the vessel's mast support structure as shown in Figure 3-5.



Figure 3-5 – Receive Monopole

Following installation, an extensive system check was carried out to ensure proper function and that all components operated as per specification.

3.4 Evaluation Activities and Resulting Data

The objectives outlined in Section 3.2 were not completely fulfilled for reasons explained as follows. First, the weather was very calm during the entire field program—a rare occurrence in South-Central Alaska in April. Consequently, there was little wave action to provide a means of assessing system performance in the presence of significant sea clutter. This makes it difficult to draw a fair comparison to the existing SeaScan™ installation since the UHF radar is designed to offer superior detectability in high sea states. Second, the backscatter levels observed on S-band were significantly less than that of L-band. This was surprising because even though less power was available for S-band (about -3dB relative to L-band), the antenna gain was 6dB higher than that of L-band. Investigation into this phenomena is on-going, including detailed assessment of the power amplifiers and antennae. Regardless of the outcome of this investigation, the lack of clutter precludes any comparison between the two bands, as the differences were expected to be manifested under severe clutter conditions.

The field evaluation revealed two specific technical issues that were well-characterized, but unfortunately not repairable in the field. The first of these was a carrier feed-through phenomena that essentially limited the dynamic range of the system (i.e. prevented use of the full range of gain, thus compromising long-range (>2km) target detection). This problem was mitigated through the use of a separate receive monopole that was less susceptible to the feed-through problem, albeit compromising antenna gain. The second problem was associated with the demodulator in the receiver. The transmitted signal saturates the receiver for a short period of time, and all components are *well-behaved* under this situation with the exception of the demodulator, which experiences drop-out, or a significant reduction in gain, for a period of about 10 μ Sec. This period is equivalent to 1500m in range. Therefore, only targets outside 1500m, or large targets inside 1500m, could be detected.

Despite these system problems, data were collected under specific scenarios that demonstrated the conceptual attributes of the system—in particular pulse compression. This section will focus on data collected from particular targets that emphasize how these conceptual attributes of the system were demonstrated.

The route taken by the vessel over the course of the field exercise is shown in Appendix B. This chart is also annotated to show the location of each of the targets used for discussion in the following sub-sections.

3.4.1 Middle Rock Navigation Marker

The performance attributes of the UHF radar, are best illustrated by small *discrete targets*, less than 5m in depth along a radial line from the antenna. This is because such a target should produce a single peak as a result of pulse compression that would clearly exemplify the resolution capabilities of the radar. The Middle Rock navigation marker at the entrance to Port Valdez, shown in Figure 3-6, is a good example of such a target.



Figure 3-6 – Middle Rock Navigation Marker

Figure 3-7 shows a small portion (4 of 251 pulses) of the L-band radar return (backscatter) in uncompressed form, in the direction of Middle Rock, from a distance of 1.03km. The four large pulses are actually the transmitted pulses that are coupled directly from the transmit antenna to the receive mono-pole and appear at just about zero-delay. Backscatter from Middle Rock is evident just following the transmit pulses. In fact, this backscatter is partially contained within the transmit pulse, which is itself 1500m in length. It is important to note that the transmitter power is only 140 watts; so all backscatter is relatively weak. The signal processing algorithm considers all 251 pulses collectively and coherently; its output, from this particular case, is shown in Figure 3-8.

The theoretical range resolution of any radar is related to its bandwidth, and in this case can be predicted as follows:

$$\Delta R = \frac{c}{2 \cdot BW} = \frac{3 \times 10^8 \text{ m/s}}{2 \cdot 25 \text{ MHz}} = 6 \text{ m}$$

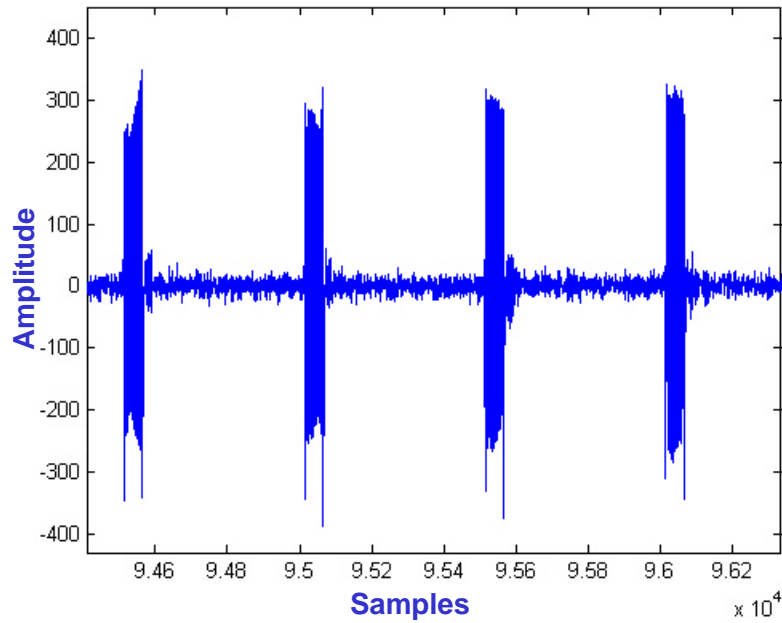


Figure 3-7 – Middle Rock, Raw Uncompressed Data

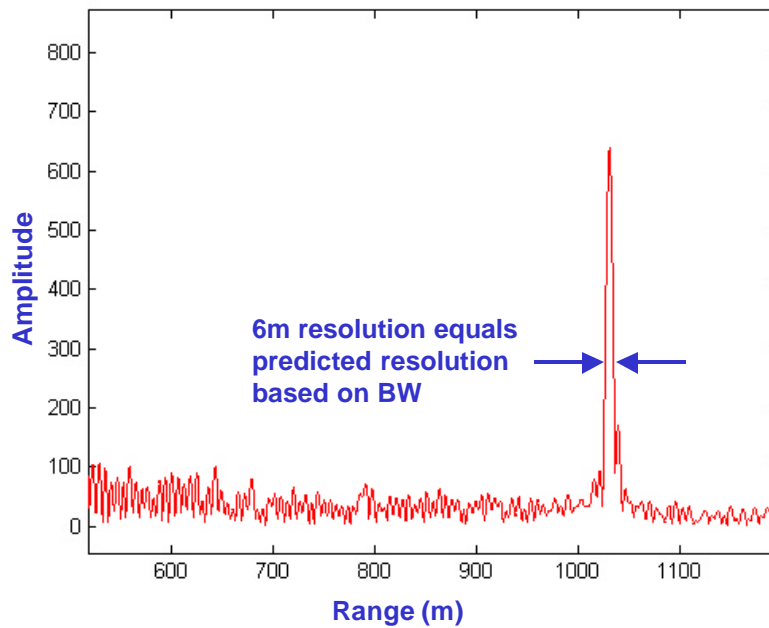


Figure 3-8 – Middle Rock, Pulse-Compressed Output

Figure 3-8 clearly illustrates that the width of the compressed pulse obtained from the Middle Rock reflection is very closely matched to the theoretical range resolution.

3.4.2 Bligh Reef RACON

A second discrete target, the Reef Island RACON Tower, was utilized to illustrate the effectiveness of pulse compression. The tower is shown in Figure 3-9, and the corresponding L-band pulse-compressed output, is shown in Figure 3-10, for a range of 665m. Again, the range resolution specification for the system was met for this target, as evident in the narrow width of the *spike* seen at 665m.



Figure 3-9 – Bligh Reef RACON

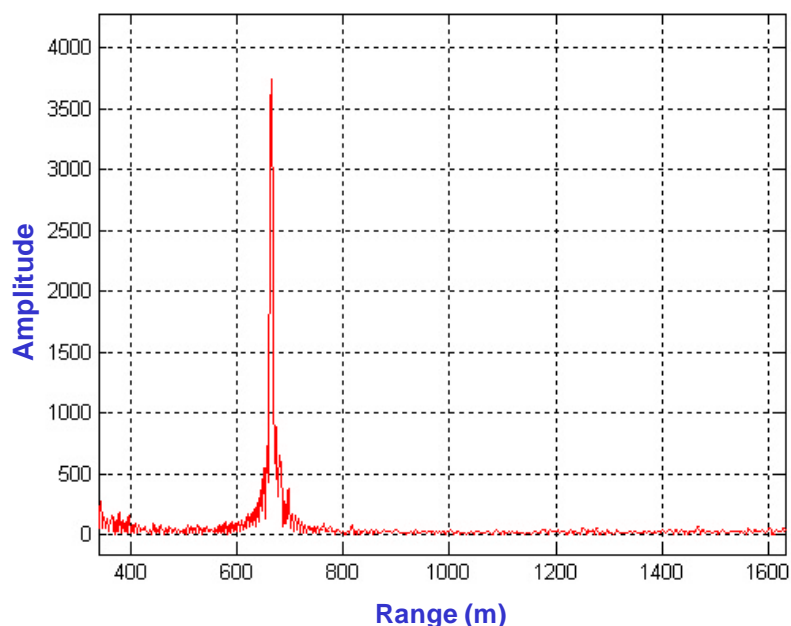


Figure 3-10 – Bligh Reef RACON, Pulse-Compressed Output

3.4.3 Iceberg Near Point Freemantle

Figure 3-11 shows an iceberg near Point Freemantle. Figure 3-12 is the pulse-compressed output from a range of 620m. The interesting observation in this example is the two closely spaced peaks in the output. This particular iceberg had an elongated shape that in effect produced multiple returns. The manner in which these returns combine is reflected in the double peak. This example illustrates the difference between a discrete target and a diffuse target. The latter does not produce a distinct spike in the output, but rather is the result of many overlapping returns. This target is actually somewhere between a discrete and diffuse target as there are clearly two distinct spikes (as opposed to the next example, which is purely diffuse).



Figure 3-11 – Iceberg near Point Freemantle (Glacier Island in Background)

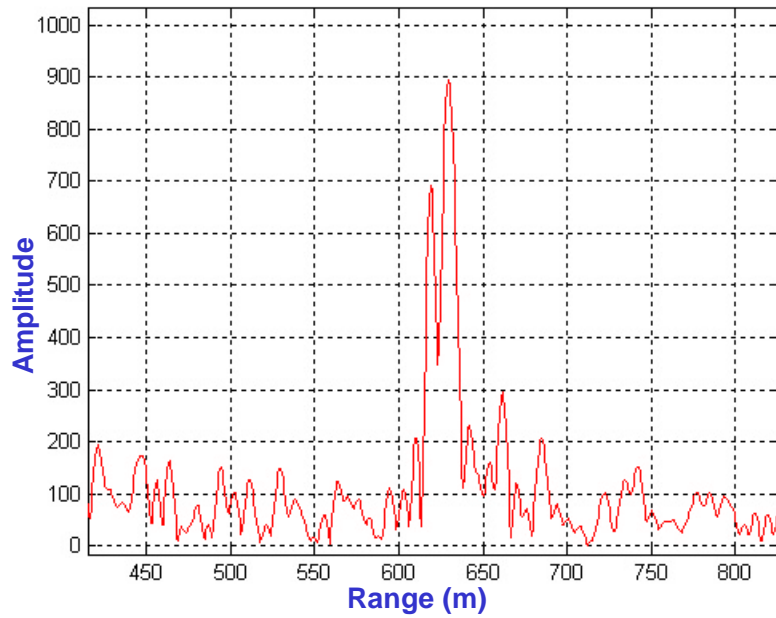


Figure 3-12 – Iceberg near Point Freemantle, Pulse-Compressed Output

3.4.4 Glacier Island from Long Range

This example presents a sample of data obtained representing backscatter from Glacier Island at a range of about 11km. It should first be pointed out that the range-periodic spikes that appear in Figure 3-13 are artifacts of carrier feed-through, and should be ignored. This figure demonstrates that although the antenna is highly directional, a large target present in the direction of a sidelobe will generate a significant return. In this case the antenna was pointed away from Bligh Island; however, it did appear strongly in the output. The most notable observation is the target observed at about 11km – Glacier Island. With little more than 100 Watts of transmitted power, the system was able to see this (albeit large) target at long range. Whereas the last two examples demonstrated the resolution achievable through pulse compression, this example exemplifies the ability to recover and display very weak signal returns.

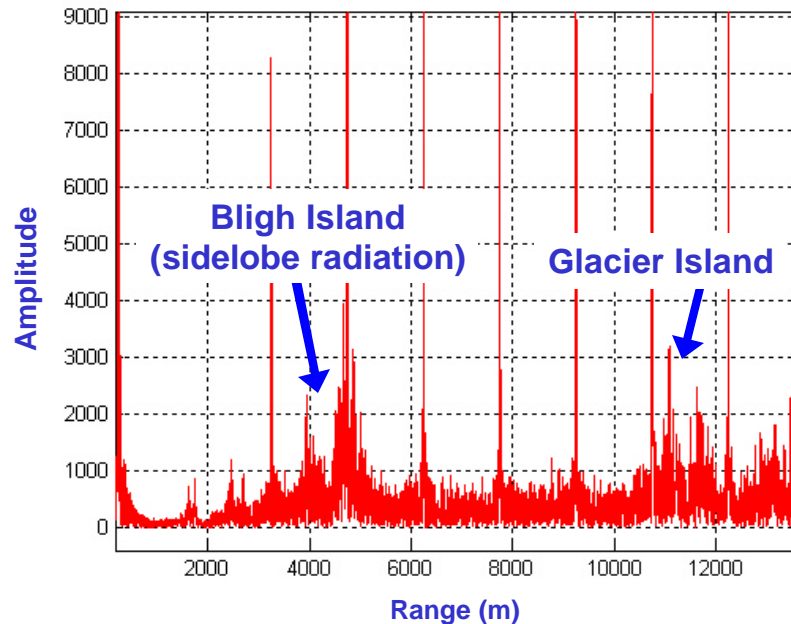


Figure 3-13 – Glacier Island, Pulse-Compressed Output

3.4.5 Experimental Summary

Although many other radar targets were utilized over the course of the field program, and much data was collected, the particular examples highlighted in this section best illustrate the characteristics of coherent SFM that were made evident as a result of the work. The navigation marker and the RACON cases demonstrate the power of pulse compression in

terms of improvements in signal-to-noise ratio and the achievable fine resolution. The iceberg case is an example of how high-resolution radar can provide more detail as to the nature or physical make-up of the target. This could be useful in target classification for instance. Finally, the Glacier Island case shows how very weak signals from long-range targets can be detected using pulse compression. This feature permits the use of an inexpensive low-power high-quality amplifier for most applications. The cost of coherent processing would dramatically increase if a high-power amplifier of high quality were required.

4 DATA ANALYSIS AND SIMULATION

4.1 Radar Model

Most aspects of the operational UHF radar were simulated through a customized model programmed in MATLAB® script. This model has been an invaluable aid in understanding the theoretical performance limitations of the radar design as well as a tool in performing system diagnostics. A portion of the same model was also used to post-process the real acquired radar returns, which facilitates a fair comparison with simulated data.

Figure 4-1 shows a sample of simulated output corresponding to a radar configuration identical to that of section 3.4.2. Comparison with Figure 3-10 reveals that the real radar output acquired from the RACON tower is very similar to the simulated result, particularly the resulting pulse-width (note that the differences in vertical scale and range offset are irrelevant).

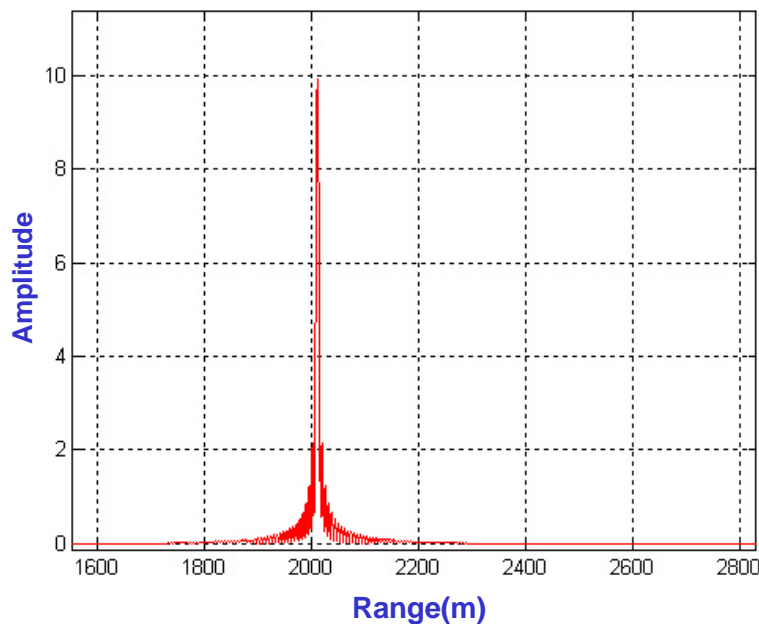


Figure 4-1 – Simulated Pulse-Compressed Output

4.2 Doppler Processing

Doppler processing is a powerful means of extracting more information from a radar return. As a target moves towards, or away from, the antenna, radio waves are compressed or stretched respectively, resulting in a frequency shift between the

transmitted waveform and the reflected waveform; this shift is referred to as a Doppler shift. Time-domain processing does not reveal this information; however, utilizing the frequency domain provides for further separation of targets moving at different velocities. Since reflections from oceans waves (clutter) are also subject to Doppler shifts, Doppler processing can enhance one's ability to distinguish a real target from clutter.

Earlier work on UHF radar (Power and Randell, 1999) utilized Doppler processing in the manner described above to improve the detectability of targets in clutter. A key element in this processing is Doppler resolution. Improved Doppler resolution is essentially obtained through increasing the duration over which a signal is transmitted, either by increasing the number of pulses or increasing the pulse width (this varies depending on the exact method employed). For instance, in the simple case of a single pulse, the Doppler frequency resolution is

$$\Delta f_D = \frac{1}{t_p}$$

where,

t_p = pulse-width

and the corresponding velocity resolution is

$$\Delta v = \frac{c\Delta f_D}{2f_0}$$

where,

f_0 = frequency of transmission

c = speed of light

The earlier work on UHF radar obtained its velocity resolution through the processing of many pulses, and achieved a Doppler resolution of

$$\Delta f_D = \frac{1}{N_p T}$$

where,

N_p = number of pulses

T = pulse repetition period

For 2096 pulses and a repetition rate of 500Hz, this translated to a Doppler resolution of 0.239Hz, or 0.15 knots.

The current form of the coherent radar was configured to investigate the concept of pulse compression. This meant that given the available bandwidth, the number of pulses and the pulse-width were restricted to optimize pulse compression. This particular configuration allowed for only 341 pulses (S-band), with a repetition rate of 10000Hz, rendering a Doppler resolution of 29.3Hz, or 3.6 knots. The dominant Doppler peaks, known as Bragg peaks (Power and Randell, 1999), occur below 10Hz. Therefore, this resolution is insufficient for the task of distinguishing moving or stationary icebergs targets from clutter in the Doppler domain. It's important to note that inability of the radar to render sufficient Doppler information is not a consequence of the modulation scheme employed or the signal design, but rather a limitation of hardware that can be easily overcome through the incorporation of an embedded processor for precise timing of multiple sweeps.

Further development of the coherent radar would consider signal configurations that optimize target detection using both temporal and Doppler domains. The necessary signal configuration can be achieved by introducing an embedded micro-controller to the system that enables precise timing of multiple triggers of the radar sweep.

5 CONCLUSIONS AND RECOMMENDATIONS

This field program was challenged by two particular technical problems—carrier feed-through and demodulator drop-out—that combined to limit the scope and range of targets that could be used in the study (buoys and small icebergs within the 500-2000m range). However, with the limited data, the theoretical system attributes were demonstrated and verified. Additionally, the technical problems were well-characterized and understood, so that system performance following the remedy of these problems is predictable. This will facilitate a high probability of greater success for the next iteration of development.

The key elements of pulse compression were clearly illustrated in the ability to recover the weak returns from a meager 100W transmitter and the ability to determine the position of a target to a resolution of 6m.

It is recognized that extending the signal design from a single SFM sweep to a synchronous multiple sweep (i.e. repeating the current signal transmission many times, as accomplished by the previous UHF radar prototype) will improve target detectability at long range or small target detectability in general. Furthermore, multiple sweeps can be utilized to improve Doppler resolution, thus enhancing the ability to distinguish targets from clutter. The 1999 RCAC report on the earlier version of the UHF radar (Power and Randell, 1999) demonstrated how powerful such processing can be in improving target detectability. Synchronous multiple sweeping can be accomplished through the use of an embedded micro-controller to provide the precise timing requirements needed by this method of transmission. In the current design, the PC triggers each transmission sequence, and can not be relied upon for such precise timing. The micro-controller will also bring other benefits to the design such as:

1. power-level equalization and maximization across the transmission band;
2. ability to impart more sophisticated coding to reduce correlator artifacts (e.g. Barker Coding).

Observations of the effects of antenna sidelobes were significant, and warrant further investigation into antenna design. The design theoretically yields sidelobes at -13dB relative to the main lobe, as was verified through lab measurements. However, the presence of large targets, such as land masses, in the vicinity of the sidelobes, can mask out returns from very small targets in the broadside direction. Investigation into means of alleviating sidelobe effects are important from an operational perspective of the coherent UHF radar. One approach is to employ a standard radar scanner that utilizes antenna beamshaping to suppress sidelobes. For this work, careful selection and use of the

environment surrounding targets of interest mitigated sidelobe problems during the field evaluation; this approach would not be effective in an operational mode. Further antenna research is also needed to widen the bandwidth. The advantages of pulse compression witnessed during this field program would be enhanced with more available bandwidth—so this aspect of antenna design is very important.

Installation aboard the research vessel Auklet went very smoothly, and this vessel proved to be ideal for the purposes of the field trial. The mounting of the antenna, location of the radar transceiver and routing of the coaxial feeds were well facilitated by the vessel. The navigational expertise and cooperativeness of the operator and familiarity with the region proved invaluable throughout the entire exercise.

This project facilitated significant progress in the development of an advanced radar specialized for small-target detection in high sea states. Demonstration of the key attributes of SFM was the most significant outcome of this field program, and the identification and characterization of several system issues will assist tremendously in refining the UHF radar throughout the next iteration of development. The work has also drawn focus to the particular elements of the system which need most attention. The next logical step is to incorporate the improvements identified thus far, and repeat the field work in the presence of significant clutter. C-CORE remains confident that coherent processing in the UHF band is key to improving the state-of-the-art for detecting small targets in clutter, and will actively pursue further development of the coherent UHF radar.

REFERENCES

Power, D. and Randell, C. (1999) "UHF Radar, Prince William Sound Field Program Final Report." Contract Report for the Regional Citizens' Advisory Council, Valdez, AK, C-CORE Contract Number 99-C32.

Rossiter, J. R., Guigné, J., Hill, C., Pilkington, R., Reimer, E., Ryan, J., and Wright, B., 1995 "Remote Sensing Ice Detection Capabilities – East Coast," Environmental Studies Research Funds, Report No. 132.

APPENDIX A – GRAPHICAL USER INTERFACE

Fi Radar Controller

Main

DD51

Lo Frequency (MHz) : 5

Hi Frequency (MHz) : 39

Frequency step (MHz) : 0.1

Step period (us) : 100

I : 4095

Q : 4095

DD52

Lo Frequency (MHz) : 5

Hi Frequency (MHz) : 39

Frequency step (MHz) : 0.1

Step period (us) : 100

I : 4095

Q : 4095

Demod

LO Frequency (MHz) : 91.25

Main clock frequency Frequency (MHz) : 10

DAQ Pulse width (us) : 10

PLL1

L-Band

Registers

R (15-bit) : 100

A (6-bit)* : 12

B (12-bit)* : 234

CP (3-bit) : 2

Freq (MHz)* : 750

Pre-scaler

8/9

16/17

32/33

64/65

Reg calc

Freq calc

S-Band

Registers

R (15-bit) : 100

A (6-bit)* : 0

B (12-bit)* : 750

CP (3-bit) : 4

Freq (MHz)* : 2400

Pre-scaler

8/9

16/17

32/33

64/65

Reg calc

Freq calc

Band select

L-Band

S-Band

Shutdown

* Can be entered or calculated

PLL2

L-Band

Registers

R (15-bit) : 100

A (6-bit)* : 8

B (12-bit)* : 206

CP (3-bit) : 5

Freq (MHz)* : 660

Pre-scaler

8/9

16/17

32/33

64/65

Reg calc

Freq calc

S-Band

Registers

R (15-bit) : 100

A (6-bit)* : 28

B (12-bit)* : 721

CP (3-bit) : 4

Freq (MHz)* : 2310

Pre-scaler

8/9

16/17

32/33

64/65

Reg calc

Freq calc

* Can be entered or calculated

AGC Offset (dB) : 0

Constant gain (V) (Uses AGC if zero) : 1.5

AIN Gain : 1,2,5,10,20,50

Gate delay (us) : 50

Use Daq

Trigger end delay (ms) (if not using DAQ) : 0

Hold reset

CW Enable

Exit

Master Reset

Send

Trigger

Multi Trigger

Pulse Train

APPENDIX B – VESSEL ROUTE

